Structural Design of a Modular Aircraft

Mafalda Joana Bayan Ferreira Magro
mafalda.magro@tecnico.ulisboa.pt

Instituto Superior Técnico, Universidade de Lisboa, Lisbon, Portugal

February 2020

Abstract

Nowadays, the transportation sector faces a lot of challenges in meeting the growing demand for common passengers mobility while reducing traffic, improving safety and mitigating emissions. Automated driving and electrification are disruptive technologies that may contribute to these goals, but they are limited by congestion on existing roadways and land-use constraints. Due to this, the interest of society in electric or hybrid Vertical Take-Off and Landing (VTOL) aircraft, that can basically act as flying cars, has grown significantly. This peculiar type of aircraft may overcome the limitations of congestion and land-use by enabling urban and regional aerial travel services with the need of much smaller infrastructures when compared with conventional aircraft. Said so, this work consists in the development of a parametric design methodology of the lifting system (wing-tail) of a VTOL aircraft, on behalf of the Flexcraft's project, for its critical flight conditions. Using the commercial software ANSYS it is possible to perform finite element analyzes and develop a methodology to perform structural parametric studies with the main objective of minimizing the weight without compromising its structural integrity, i.e. not exceeding the material yield strength and the maximum deflection defined for the wing and stabilizer.
Keywords: VTOL, FEA, FEM, Parametrization, Flexcraft

1. Introduction

The Flexcraft project, whose name appeared as an abbreviation for Flexible Aircraft, arose due to the emerging interest in transforming the way people travel. This concept born from the NewFACE's project and is being developed by ALMADESIGN, Instituto Superior Técnico (IST), Sociedade de Engenharia e Transformação S.A. (SETsa), Embraer Portugal S.A. and Instituto de Ciência e Inovação em Engenharia Mecânica e Engenharia Industrial (INEGI). The Flexcraft combines the idea of modularity and flexibility, because this aircraft is composed by a lifting system capable of disengage from the fuselage module, allowing the cabin reconfiguration for different missions (commercial and recreational, emergency and assistance, among others), through short runway operation, improving the overall performance. Several innovative configurations have been proposed throughout the various phases of the project, but this work is focused on the structural behavior of the lifting systems (wing-tail) of the Flexcraft VTOL configuration when submitted to the flight loads, specially on the critical points of the flight envelope.

The main objectives of this work are the structural analysis using the Finite Element Method (FEM) of the Flexcraft VTOL configuration lifting system and the development of a model that can be used to improve an initial estimation of the aircraft's geometry.

2. Flexcraft

After identifying all the requirements imposed by the project consortium (Table 1), it is mandatory to analyze other types of aircraft in the market and identify what can be improved. Due to this, the Utility, Tandem Wing and the Flying Wing configurations are considered.

Table 1: Project Requirements.

Requirements	
Range [km]	1000
Passengers	9
Payload [kg]	900
Specifications	
Cruise Speed [km/h]	400
Cruise Altitude [ft]	6000
Take-off and Landing Distance [m]	< 325
Rate of Climb [ft/min]	1200
Stall Speed [kts]	< 61
Configuration	
Power Train	Series or Parallel
Lifting System Type	STOL or VTOL

To make sure that all the requirements are met and after a careful analysis and deliberation of the characteristics of each configuration, the consortium opted for the Utility concept. With that being

Table 2: Utility VTOL concept characteristics. [1]

Part	Parameter	Value
Global	MTOW [kg]	4500
	C_{m_α}	-0.57
	C_{n_β}	0.18
	Fuel mass [kg]	440
	Wiring mass [kg]	215.94
	Batteries mass [kg]	419.78
	Systems mass [kg]	95.20
	2 Booms mass [kg]	92.46
	Turbogenerator mass [kg]	121.30
	Static margin [%]	10
Fuselage	Length [m]	6.2
	Diameter [m]	1.6
	Capacity	9 pax
Main wing	Mass [kg]	377.92
	Span [m]	15
	Wing area [m^2]	35.8
	Chord root [m]	3.4
	Chord tip [m]	1.36
	Mean chord [m]	2.4
	AR	6,3
	Airfoil	NACA64A415
	Twist	NA
Horizontal Tail	Mass [kg]	15.86
	Span [m]	4
	Chord [m]	1.86
	Airfoil	NACA0009
Vertical Tail	Mass [kg]	16.36
	Span [m]	2
	Chord	1.14
Engines	Propeller diameter [m]	1.4
	Propeller power [kW]	410
	Leading Edge 4 engines mass [kg]	411.07
	Trailing Edge 4 engines mass [kg]	411.07

said, the development of this work is focused on the VTOL Utility configuration (Figure 1). The main characteristics of the aircraft are presented in Table 2.

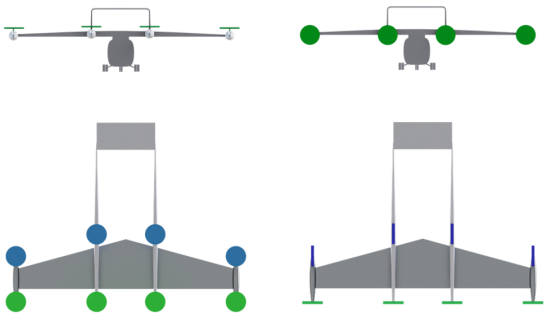

Figure 1: Flexcraft front and top view: Take-off on the left and Cruise on the Right.[1]

3. Methodology

In the following Section, all the methodologies used during this work are defined.

3.1. Structural Analysis

An aircraft structure is required to support ground and air loads. The first includes all the loads encountered during its movement on ground (taxiing and landing loads, towing and raise up) and the second one include loads imposed on the structure during flight by manoeuvres and gusts conditions. Normally, when flying, direct loads, bending, shear and torsion occur in all parts of the structure in addition to local, normal pressure loads imposed on the skin.

To ensure that an aircraft withstands all these loads, several types of computational analysis can and should be performed prior to the manufacturing. During this work, the types of analyses performed are essentially Static and Inertial, with the the main goal of making parametric studies, with changes on the thickness, size and number of several of the aircraft structural components.

3.2. Finite Element Method

To perform the structural analysis of the wing-tail structure, a numerical approach used worldwide to solve complex engineering problems, the Finite Element Method (FEM), is used. In this method, the original body of the structure is approximated by the assemblage of smaller similar areas, known as the Finite Elements (FE), interconnected with each other [3].

The FEM became so popular because it allows to simulate any system and to determine desired properties with accuracy before experimental tests, fabrication and manufacturing, reducing costs. This is also a very good approach for complex models, where exact or theoretical solutions are really difficult to obtain.

Since the main goal of this work is to make parametric studies of the aircraft structure, Ansys Parametric Design Language (APDL) is the environment chosen to make the computational simulations.

3.3. Finite Element Models

The Flexcraft's wing-tail structure is composed by several different components, such as the ribs, spars, booms, skin, engines, and so on, meaning that there is the need to select proper FEs according to each one of these structures. For this work, and taking into account the structures that compose the Flexcraft wing-tail structure, three different types of FEs are chosen: a Beam FE, a Shell FE and a Mass FE.

Due to the complexity of the aircraft, three models are tested: one using only Beam and Mass FE, other using only Shell FE and Mass FE and the more complex one using a combination of Beam, Shell and Mass FE.

3.3.1 Beam Geometric Model

The first model developed uses only the BEAM FE (namely the BEAM198 which is based on the Timoshenko beam theory [7]) to represent all the structures and the MASS FE (MASS21) to represent all the non-structural components which are rigidly at-

tached to the wing and stabilizer - Figure 2. This model is the Beam Geometric Model (BGM).

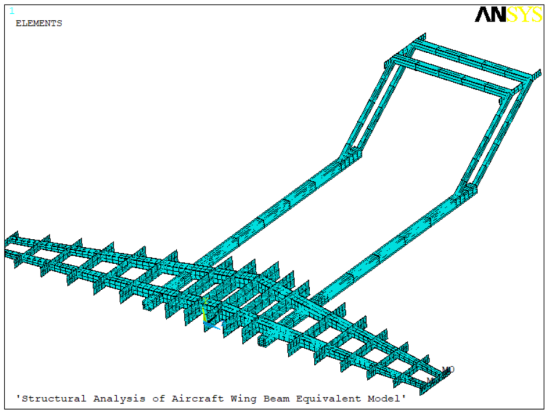

Figure 2: Beam Geometric Model developed.

This is the simplest model developed during this work and it represents only the internal structure of the Flexcraft. Since it is built only using Beam FEs, it is not possible to model the skins of the wing and stabilizer, as well as shaping the ribs with an airfoil format. The wing reinforcements can not also be represented.

All the variables defined for the BGM are shown in Table 3, along with a brief description of each one.

Input	Description
RibsIn	Number of wing ribs on the inner side
RibsOut	Number of wing ribs on the outer side
NELEM	Reducing this value increases the mesh granularity
t_in	Thickness of the wing root rib [m]
t_out	Thickness of the wing tip rib [m]
t_wingboom	Thickness of the wing spars' cross section [m]
chord_percentage	Side of the spars cross section by $d = c_{local} \times chord\_percentage$
size_rearboom	Cross section side of the boom connecting the wing to the tail [m]
t_rearboom	Cross section thickness of the boom connecting the wing to the tail [m]
size_vertical	Cross section side of the vertical boom [m]
t_vertical	Cross section thickness of the vertical boom [m]
t_ribs_tail	Cross section thickness of the tail ribs [m]
t_spars_tail	Cross section thickness of the tail spars [m]
size_spars_tail	Cross section side of the tail spars [m]

Table 3: Inputs for the Beam Model.

3.3.2 Shell Geometric Model

The second model developed during this work is the Shell Geometric Model (SGM) and, as the name itself refers, uses only Shell FEs to represent the aircraft structure. The Shell FE used is the SHELL281 (element formulated based on the Reissner-Mindlin plate theory [12]) and the MASS21 FE is used to represent all the punctual masses. When compared with the previous model, this one has the advantage of better representing the aircraft geometry, since it allows to design the ribs with an airfoil shape and also allows the representation of the wing and tail skin.

The internal structure of the wing is represented in Figure 3 and the list of variables used with a brief description are shown in Table 4.

Table 4: Inputs for the Shell Model.

Input	Description
RibsIn	Number of wing ribs on the inner side
RibsOut	Number of wing ribs on the outer side
aesize	Reducing this value increases the mesh granularity
t_in	Thickness of the wing root rib [m]
t_out	Thickness of the wing tip rib [m]
t_wingshell	Thickness of the wing skin [m]
chord_percentage	Used to define the thickness of the spars by $t\_spar(z) = c(z) \times chord\_percentage$
t_rearboom	Thickness of the booms connecting the wing to the tail [m]
t_vertical	Thickness of the vertical beams [m]
t_spars_tail	Thickness of the tail spars [m]
t_ribs_tail	Thickness of the tail ribs [m]
t_skin_tail	Thickness of the tail skin [m]

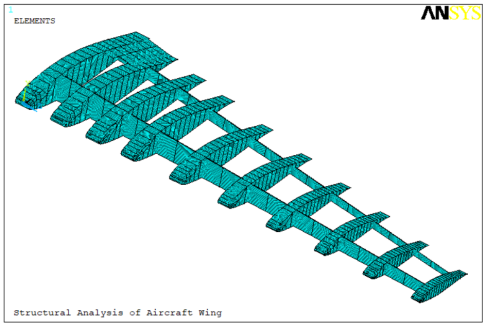

Figure 3: Internal structure of the wing for the SGM.

3.3.3 Beam-Shell Geometric Model

This is the last model developed and it is a mixture of the previous two - Figures 4 and 5 (where the beam and shell elements are presented, respectively). Since there are structures that clearly behave more as a beam, such as the spars and booms, and others that behave more as a shell, such as the skin and ribs, this last model has the main goal of obtaining a structural behavior more similar to the real aircraft. This way, and following the work previously done, the FEs used are below identified:

- BEAM189: used to model the Spars and Connection Booms;
- SHELL281: used to model the Ribs and Skins;
- MASS21: used to represent all the components as mass points rigidly attached to the wing and stabilizer.

Once again, there are several inputs that must be given to the APDL script, before making the simulation. These values will change the geometry of the model, in order to understand how each one influences the structural behavior. These variables are presented in Table 5, along with a brief description of each one.

3.4. Aerodynamic Loading

To perform the structural simulations, it is necessary to apply the aerodynamic forces acting on

Input	Description
RibsIn	Number of wing ribs on the inner side
RibsOut	Number of wing ribs on the outer side
aesize	Reducing this value increases the mesh granularity
t_in	Thickness of the wing root rib [m]
t_out	Thickness of the wing tip rib [m]
t_wingshell	Thickness of the wing shell [m]
t_wingboom	Thickness of the wing spars' cross section [m]
t_reinforcement	Thickness of the wing reinforcement's cross section [m]
chord_percentage	Side of the wing spars cross section by $d = c_{local} \times chord\_percentage$
size_rearboom	Cross section side of the boom connecting the wing to the tail [m]
t_rearboom	Cross section thickness of the boom connecting the wing to the tail [m]
size_vertical	Cross section side of the vertical boom [m]
t_vertical	Cross section thickness of the vertical boom [m]
t_spars_tail	Define the thickness of the tail spars [m]
size_spars_tail	Define the side of the tail spars [m]
t_ribs_tail	Cross section thickness of the tail ribs [m]
t_skin_tail	Define the thickness of the tail skin [m]

Table 5: Inputs for the Beam-Shell Model.

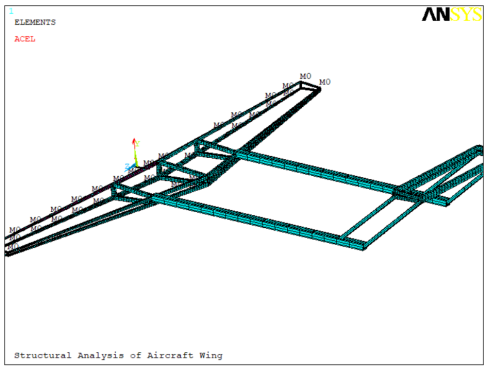

Figure 4: Internal Structure BSGM.

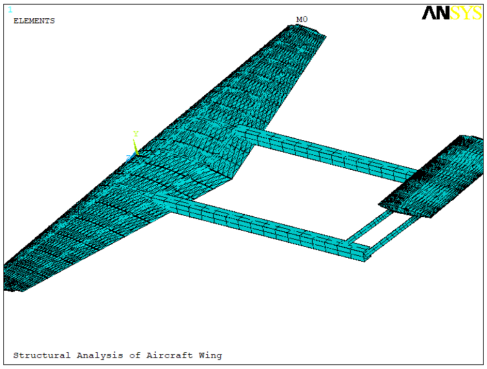

Figure 5: External Structure defined with BEAM189 FE.

the aircraft. Calculating these forces is not under the scope of this study, so they are calculated using a Multidisciplinary Design Optimization (MDO) framework [2] already developed, made for conceptual design and analysis of new aircraft configurations. The aerodynamic model of this MDO framework allows the preliminary analysis of the aerodynamic loading that an aircraft is facing.

In this work, the same aerodynamic model is used to generate the loads for the three structural models (BGM, SGM and BSGM). This tool is based in a potential flow model - inviscid and irrotational (for more details regarding this flow model see [9]). Since the lift is the largest aerodynamic load faced by the aircraft, in the upper and lower limits of the flight envelope, only the main wing and horizontal tail are considered when applying the aerodynamic model, reducing the modeling complexity of a full 3D mesh. The main limitation of this assumption is not considering the propellers mounted ahead of the wing, which would slightly increase the lift on the wing (thus lift is slightly underestimated in the aerodynamic model used). Considering the propellers would involve more complex aerodynamic effects, which can not be predicted using this 3D panel method. Concerning the horizontal tail, this is a conservative approach, since the effect caused by the wing wake is not accounted. This effect would lead to a lower Lift force, meaning that the value obtained for the horizontal tail is slightly overestimated.

This model uses the 3D panel numerical method described by [9], with compressible corrections (which in this case are not applied since the cruise speed of the Flexcraft is approximately Mach 0.3) and viscous friction corrections.

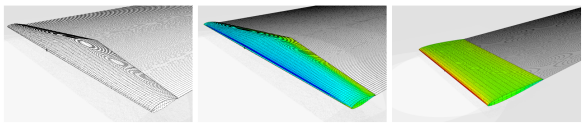

Figure 6: MDO framework results: (a) Wing Mesh. (b) Wing (n_{max}). (c) Horizontal tail (n_{min})

An illustration of an aerodynamic mesh for the main wing can be seen on Figure 6 (a) alongside with two illustrative simulations of the maximum and minimum load factors for main wing and horizontal stabilizer, respectively - Figure 6 (b) and (c).

3.5. Structural Improvement Model

Since the Geometric Models are prepared for parametric studies, it is possible to take advantage of it and try to optimize the variables defined for the BGM, the SGM and the BSGM. Due to this, a model that runs on top of the Geometric Models, with the main goal of obtaining a lower weight for the structure, is built - the Structural Improvement Model (SIM) - Figure 7. With the objective of achieving a lightweight structure, a upper limit target value of $1500kg$ (which corresponds to a $1/3$ of the total MTOW defined) is set.

Essentially, this model starts from a set of i variables, defined for each Geometric Model, with over-dimensioned values that produce an overweighted and over-robust structure. Having this initial set of values, it is then necessary to define the minimum (var_i^{min}), maximum (var_i^{max}) and incremental (var_i^{inc}) values that will be analyzed for each variable, var_i.

Since the parameter sequence influences the results obtained, it is necessary to find a way to decide which variable to analyze first. Thus, as the main objective is to minimize the structural weight,

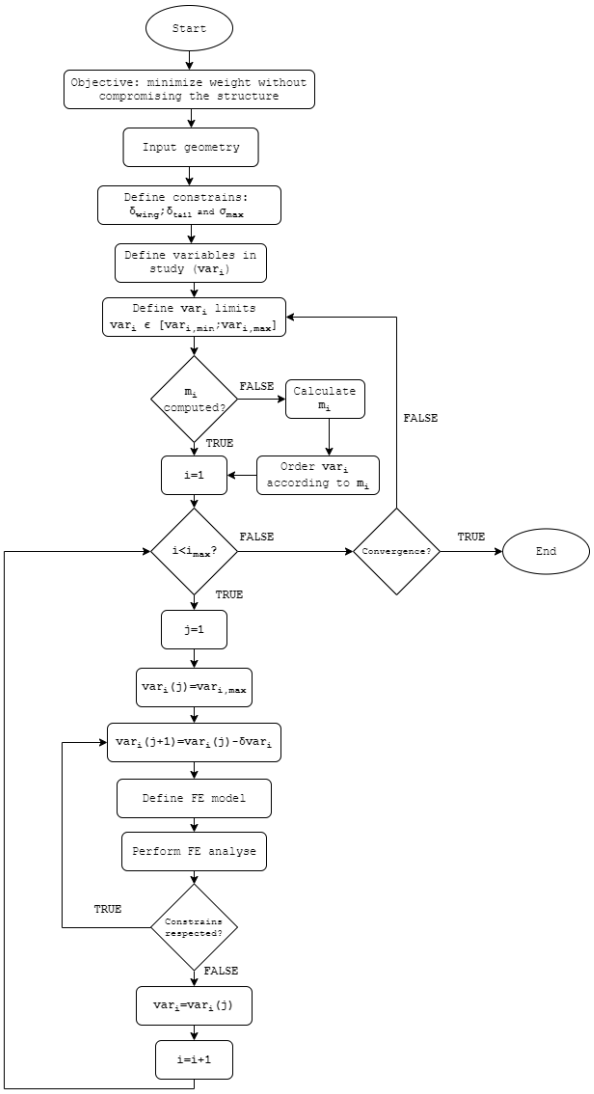

Figure 7: Structural Improvement Model - SIM.

W, it is fundamental to verify the influence of each variable on it. Said so, the weight variation factor (m_i) is calculated for each variable. This value represents the sensibility of the weight variation with the change of each variable, in kg/m.

After defining this, it is necessary to define some constrains. These constrains can be geometric or structural, according to the needs and specifications of the project.

After defining all the needed values and the constrains, the model increments one or two variables at a time, depending on the structural component in study. For each increment, a FEA is performed and all the values for the constrains are obtained. Then, during the post-processing phase, the value for var_i that minimizes the weight while fulfilling the constrains is fixed and used for the next variable's parametric study.

The total number of simulations performed, N_{par}, can be calculated by

$$N_{par} = \left[\sum_{i=1}^{n} \left(\frac{var_i^{max} - var_i^{min}}{var_i^{inc}} + 1 \right) + \sum_{i=1}^{n} \left(\frac{var_{i,1}^{max} - var_{i,1}^{min}}{var_{i,1}^{inc}} + 1 \right) \times \left(\frac{var_{i,2}^{max} - var_{i,2}^{min}}{var_{i,2}^{inc}} + 1 \right) \right] \times 3 \quad (1)$$

Please note that it is necessary to divide the equation in two different blocks: the first block calculates the number of simulations for each variable studied individually, while the second block refers to the case when two variables must be studied together. This last case happens for every hollow cross section, where the variation of thickness and side must be evaluated at the same time.

3.6. Parametric Constrains

As stated in Subsection 3.5, in order to run the SIM, it is necessary to define some constrains. Even knowing that the main goal of the SIM is to reduce the weight of an initially oversized model, that is still capable of withstanding all the aerodynamic loads, without structural failure, one must ensure that the aircraft remains aerodynamic efficient, even when operating in critical conditions. This means that, even for the limiting load factors, the structure must not present high deformations.

With that being said, it is necessary to define some constrains in order to obtain suitable values for the structure. On this specific study, the main constrains are the maximum stress (σ_{max}), the Wing Tip Displacement ($\delta_{wingtip}$) and the Tail Displacement (δ_{tail}). Regarding σ_{max}, the constrain is defined by

$$\sigma_{max} < \frac{\sigma_{yield}}{SF}, \quad (2)$$

being σ_{yield} the yield stress of the material, i.e., the elastic limit of the material and SF a Safety Factor. A $SF = 1.5$ is selected, since it is the normal value used for passenger aircraft structural design. This safety factor alone is equivalent to a probability of failure of between 0.01 to 0.001 [8].

For $\delta_{wingtip}$, a high wing stiffness is considered, meaning that its value can not be higher that 5% of the wingspan [6]. Regarding the tail displacement, and due to its important role in ensuring the aircraft stability, it was considered that its value could not also be higher than 5% of the distance between the tail and the leading edge's spar (d_{wt}). Mathematically, these conditions are defined by

$$-0.05b \leq \delta_{wingtip} \leq 0.05b, \quad (3)$$

$$-0.05d_{wt} \leq \delta_{tail} \leq 0.05d_{wt}. \quad (4)$$

having b and d_{wt} the values of 7.5 m and 9.25 m, respectively.

3.7. Material Selection

Choosing a material, in the aerospace industry, may require an extensive evaluation of its performance under creep, tension, compression, bending, fatigue and corrosion. Nowadays, there are different options to fulfill the requirements of a new aircraft project: metals, composites, wood, among others [13].

The wing structure of a modern aircraft can be designed with a combination of different types of materials, according to their specific structural function. Each of these components needs to support different loads and so the right material needs to be selected. Steel or aluminium alloys can be used in the ribs and spars manufacturing, while composite materials are common in the design of the wing skin and the control surfaces.

For simplicity, an Aluminium alloy, which properties are presented in Table 6, is chosen to perform the structural analysis in this work. This metal is characterized by having lower density values compared to steel alloys, with good corrosion resistance properties [11].

Table 6: Aluminium alloy properties [10]

E [MPA]	σ_{yield} [MPA]	ν [-]	ρ [Kg/m^3]
70	276	0.33	2700

4. Results Discussion

In this Section, all the results obtained are presented.

4.1. V-n and Gust Diagrams

Considering the data gathered for the Flexcraft, it is possible to obtain the V-n and Gust Diagrams (Figure 8) for its flight conditions.

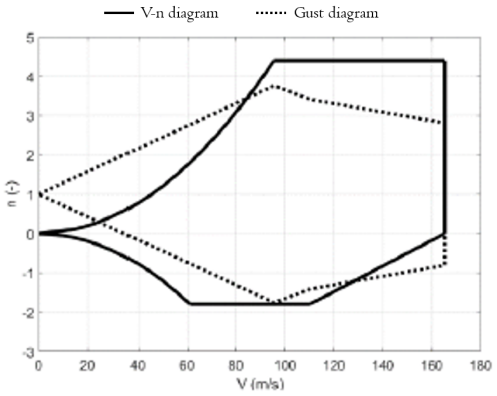

Figure 8: V-n and Gust Diagrams obtained for the Flexcraft at cruise altitude

The limiting load factors in the combined diagram are then $n = -1.8$ and $n = 4.4$, as defined in [5], for an utility aircraft, with an air flow velocity of $400km/h$ and an angle of attack of 6^o and -6.65^o, respectively.

4.2. Convergence of the Geometric Models

Before starting the computational simulations, it is mandatory to make a mesh convergence study, for each of the FE models developed. This is a crucial step. If the FEM is applied using a non-converged mesh, the solutions obtained might be erroneous, which can lead to wrong design decisions and disastrous consequences [4].

For the models in study, the two parameters that control the mesh refinement are the NELEM (represents the number of subdivisions for each Beam FE, meaning that increasing this value increases the mesh refinement), for the Beam Geometric Model, and the AESIZE (represents the approximate area value of each Shell FE, meaning that reducing this value increases the mesh granularity), for the Shell and Beam-Shell Geometric Models. By refining the FE mesh and analyzing the results, the values selected are the following:

- $NELEM = 5$, for the Beam Geometric Model, which corresponds to 573 elements for the structure in study. The average relative error, when compared with the more refined mesh, is 0.013%;
- $AESIZE = 0.5$, for the Shell Geometric Model, which is the equivalent to 3444 FEs. The average relative error, when compared with the most refined mesh, is 5.36%;
- $AESIZE = 0.5$, for the Beam-Shell Geometric Model. This value corresponds to 32392 FEs and has an average relative error of 2.93%.

A convergence study on the aerodynamic meshes of the main wing and horizontal stabilizer is also done, resulting in meshes with 50 span-wise divisions and 32 chord-wise divisions that have relative errors in lift under 1%.

4.3. Beam Geometric Model

In this Subsection, the results related with the BGM, are presented. Since the aircraft behaves differently for its two limiting load factors, $n = 4.4$ and $n = -1.8$, the results for these two flight conditions must be considered.

As stated, to run the SIM, it is necessary to define an initial set of values for all the parameters. This initial values can be seen in the column I_0 of Table 7. The results for two iterations after running the SIM are also presented in Table 7.

Table 7: Beam Model - Final values for the variables.

i	var_i	I_0	I_1	I_2	Final Variation [
1	t_wingboom [m]	0.0100	0.0040	0.0024	-76 %
2	chord_percentage [-]	0.1000	0.1200	0.1600	60 %
3	t_rearboom [m]	0.0500	0.0100	0.0040	-92 %
4	size_rearboom [m]	0.2500	0.3000	0.3750	50 %
5	t_in [m]	0.0100	0.0030	0.0030	-70 %
6	t_spars_tail [m]	0.0100	0.0050	0.0010	-90 %
7	size_spars_tail [m]	0.2000	0.1750	0.1750	-12 %
8	t_out [m]	0.0050	0.0040	0.0040	-20 %
9	t_vertical [m]	0.0050	0.0020	0.0020	-60 %
10	size_vertical [m]	0.1200	0.1400	0.1400	17 %
11	t_ribs_tail [m]	0.0200	0.0080	0.0075	-63 %

The results of the constrains, obtained for the final values of the variables, can be seen on Table 8.

Table 8: Beam Model - Final results.

n	Constrain	I_0	I_1	I_2	Final Variation
-1.8	$\delta_{wingtip}$ [m]	-0.126	-0.159	-0.109	-13 %
	σ_{max} [MPa]	110.27	177.47	180.82	64 %
	δ_{tail} [m]	-0.311	-0.419	-0.441	42 %
4.4	$\delta_{wingtip}$ [m]	0.165	0.234	0.164	-1 %
	σ_{max} [MPa]	105.81	182.03	176.74	67 %
	δ_{tail} [m]	0.119	0.298	0.361	204 %
	W [Kg]	3448.88	1237.58	811.85	-76 %

Looking into the final results, the model was able to reduce the structural weight from $3448.88Kg$ to $811.85Kg$, representing a reduction of 76.46%, without compromising the structural integrity or overcoming the boundaries of the constrains previously defined. The W obtained is clearly underestimated, since the BGM fails to represent several components, such as the wing skin, tail skin and wing reinforcements, and makes an incorrect representation of the wing and tail ribs.

Looking for the variables, it is clear that all the thicknesses were extremely overestimated, since all of them were reduced. However, it is curious to see that, to decrease W, all the size variables of the hollow cross sections were increased. Considering a simple example of a cantilever beam, with length l, and with a hollow square cross section, with size a and thickness t. The cross section has a surface, S, defined by

$$S = a^2 - (a - 2t)^2 = 4t(a - t) \tag{5}$$

which can be used to obtain the weight of the beam using

$$W = S\ l\ \rho\ g = [4t(a - t)]\ l\ \rho\ g \tag{6}$$

As it can be seen, due to being a second order variable, reducing t has a much bigger impact in weight reduction when compared with a. This fact, along with the need of satisfying the constrains, leads to the behavior identified in this study, which is the thicknesses reduction and sizes increases.

Analyzing also the stress distributions, and starting by the negative flight condition, the High Stress Point (HSP) is located at wing ribs. However, it is clear that the tail spar is also facing a stress close to the σ_{max} allowed. The spars experience higher stresses near the root and the boom near the connection with the wing. Both are expected behaviors, since both components act as cantilever beams. The vertical displacement distribution is also expected, with negative values of $\delta_{wingtip}$ and δ_{tail}.

Equally as $n = -1.8$, for $n = 4.4$ the HSP is located at the wing ribs. However, it is possible to see areas of high stress concentration at the wing and tail spar's root. The wing spars are more stressed than they are for $n = -1.8$ due to the higher magnitude of the aerodynamic loads, which provoke higher bending moments across the structure. The displacement distribution is also expected, with positive values of $\delta_{wingtip}$ and δ_{tail}.

Said so, and for the final set of variables, the critical points of the BGM are then the wing ribs, the wing spar's root and the tail spar's root. Some other locations that presented higher stress concentrations are connection points between the wing and the booms, between the booms and the vertical tails and between the vertical tail and horizontal.

4.4. Shell Geometric Model

In this Section, the results related with the second Geometric Model developed, the SGM, are presented. The initial inputs for the SIM are shown in the column I_0 of Table 9, along with the results obtained after two iterations of the SIM (I_1 and I_2). The results for W and the constrains can also be seen in Table 10.

Table 9: Shell Model - Final values for the variables.

i	var_i	I_0	I_1	I_2	Final Variation [
1	t_wingshell [m]	0.0100	0.0020	0.0019	-81 %
2	t_skin_tail [m]	0.0050	0.0025	0.0025	-50 %
3	chord_percentage [-]	0.1000	0.0060	0.0056	-94 %
4	t_in [m]	0.3000	0.2700	0.2560	-15 %
5	t_out [m]	0.2000	0.1600	0.1540	-23 %
6	t_vertical [m]	0.0200	0.0020	0.0015	-93 %
7	t_rearboom [m]	0.3000	0.3000	0.2760	-8 %
8	t_spars_tail [m]	0.0080	0.0008	0.0005	-94 %
9	t_ribs_tail [m]	0.0050	0.0035	0.0031	-38 %

Table 10: Shell Model - Final results.

n	Constrain	I_0	I_1	I_2	Final Variation
-1.8	$\delta_{wingtip}$ [m]	-0.019	-0.118	-0.123	548 %
	σ_{max} [MPa]	164.21	177.52	183.90	12 %
	δ_{tail} [m]	-0.390	-0.425	-0.461	18 %
4.4	$\delta_{wingtip}$ [m]	0.006	0.094	0.101	1673 %
	σ_{max} [MPa]	71.62	156.98	169.53	137 %
	δ_{tail} [m]	0.112	0.185	0.213	90 %
	W [Kg]	17137.16	9405.75	8890.79	-48 %

Analyzing the final results obtained, the model

reduces the structural weight from $17137.16Kg$ to $8890.79Kg$, which represents a reduction of 48%. This value is extremely high when compared with the one obtained for the Beam Geometric model, but expected. This model is built using only Shell FEs, which are normally used to modulate thin web structures. Examples of this type of components in the aircraft are the wing and tail skins, as well as the ribs. Well, in this model, all the components are being modeled using Shell FEs, which is clearly a non optimal approach, specially due to the representation of the spars and the booms. Due to the nature of this FEs, the thickness of the Shell elements representing the booms and the spars are clearly oversized, in order to compensate for the reduced capacity of the Shell elements to withstand bending loads.

However, regarding the structural representation of the components, this model is more accurate than the BGM, since it allows to represent correctly the wing and tail ribs and skin. Nevertheless, and since it is independent from the Geometric Model used, the SIM presents some good results, since it is able to reduce the weight in almost an half of the initial value, while keeping the constrains in the boundaries defined.

Using this final values for the geometric variables, it is then possible to analyze the stress and vertical displacements distributions obtained for each flight condition.

It is clear that the highest stress is obtained for the negative load factor in study. As explained previously, this is due to the fact that both the aerodynamic and structural loads have the same direction. The HSP for both flight conditions is located at the wing, near the boom connection for $n = -1.8$ and near the wing root for $n = 4.4$. Looking specifically to the wing, and due to the aerodynamic loads, it is possible to observe clearly that the wing faces higher stress in the root, decreasing progressively towards the tip. The booms have also higher stress concentrations near the connections with the wing, indicating that these are also critical points for the structure. Furthermore, the connection between the booms and vertical tail can also be considered a critical structural point.

Regarding the displacement distributions, the results are more than expected. For the negative load factor, all the displacements are negative, while for the positive load factor, all the displacements are positive. For both flight conditions, δ_{tail} is higher, in module, than $\delta_{wingtip}$.

4.5. Beam-Shell Geometric Model

Finally, the results for the BSGM are obtained. Table 11 and Table 12 presents the variables after running the SIM and their corresponding constrains.

Table 11: Beam-Shell Model - Final values for the variables.

i	var_i	I_0	I_1	I_2	Final Variation
1	t_wingshell [m]	0.0040	0.0012	0.0012	-70 %
2	t_wingboom [m]	0.0050	0.0030	0.0020	-60 %
3	chord_percentage [-]	0.0800	0.0900	0.1160	45 %
4	t_skin_tail [m]	0.0070	0.0021	0.0018	-74 %
5	t_reinforcement [m]	0.0100	0.0030	0.0020	-80 %
6	t_rearboom [m]	0.0500	0.0100	0.0040	-92 %
7	size_rearboom [m]	0.2500	0.2500	0.3250	30 %
8	t_spars_tail [m]	0.0050	0.0010	0.0004	-92 %
9	size_spars_tail [m]	0.1000	0.1500	0.2250	125 %
10	t_in [m]	0.1000	0.0400	0.0390	-61 %
11	t_vertical [m]	0.0060	0.0020	0.0012	-80 %
12	size_vertical [m]	0.1000	0.1200	0.1500	50 %
13	t_out [m]	0.0500	0.0450	0.0440	-12 %
14	t_ribs_tail [m]	0.0100	0.0020	0.0020	-80 %

Table 12: Beam-Shell Model - Final results.

n	Constrain	I_0	I_1	I_2	Final Variation
-1.8	$\delta_{wingtip}$ [m]	-0.053	-0.063	-0.060	13 %
	σ_{max} [MPa]	125.19	159.92	182.50	46 %
	δ_{tail} [m]	-0.227	-0.434	-0.418	84 %
4.4	$\delta_{wingtip}$ [m]	0.058	0.079	0.076	31 %
	σ_{max} [MPa]	159.82	183.68	180.36	13 %
	δ_{tail} [m]	0.061	0.305	0.325	432 %
	W [Kg]	5675.11	2504.33	2190.46	-61 %

Looking at the final results, the SIM was able to reduce the structural weight from $5675.11Kg$ to $2190.46Kg$, corresponding to a decrease of -61.40%. This value is quite near the goal weight of $1500Kg$, being this results discussed and compared with the previous ones in the final Subsection 4.6. However, as expected, the weight obtained falls between the weight obtained for the BGM and the SGM, since this model was built in order to use the pros from both and overcome most of the cons of each one of them. This model should produce also the most accurate results, since it allows to represent correctly all the aircraft structural components, with the right type of FE.

Using these final values for the geometric variables, it is then possible to analyze the stress and vertical displacements distributions obtained for each of the load factors in study. The higher stress for both flight conditions is quite similar, being $182.50MPa$ for $n = -1.8$ and $180.36MPa$ for $n = 4.4$, indicating that the structure is well dimensioned for both load factors.

For the negative load factor, the areas that face higher stresses are the connections between the wing and the boom, the wing reinforcement, the connection between the boom and the vertical tail and, finally, the connection between the vertical tail and the horizontal tail, where the HSP is located. For $n = 4.4$, the areas are the same, with the addition of the wing spar's root and the wing skin near it.

Concerning the displacement distributions, the results are clearly the expected. For $n = -1.8$, all the displacements are negative, while for $n = 4.4$, all the displacements are positive. For both load factors, δ_{tail} is higher, in module, than $\delta_{wingtip}$.

4.6. Final Remarks

To conclude, the results obtained after applying the SIM to each Geometric Model are compared and discussed. To a better visualization, they can be seen in Table 13.

Table 13: Comparison of the results obtained for the 3 Geometric Models

n	Constrain	BGM	SGM	BSGM
-1.8	$\delta_{wingtip}$ [m]	-0.109	-0.123	-0.060
	σ_{max} [MPa]	180.82	183.90	182.50
	δ_{tail} [m]	-0.441	-0.460	-0.418
4.4	$\delta_{wingtip}$ [m]	0.164	0.101	0.076
	σ_{max} [MPa]	176.74	169.53	180.36
	δ_{tail} [m]	0.361	0.213	0.325
	W [Kg]	811.85	8890.79	2190.46

The Beam Geometric Model, and as defined, is clearly the model that has the lowest weight, being way below the design goal weight of $1500Kg$. This is completely expected, since this is not capable of representing several components of the structure, such as the wing and tail skin and the wing reinforcement. Also, the ribs are also represented with an approximation, making it quite inaccurate.

Regarding the Shell Geometric Model, the weight obtained is clearly oversized. This model allows a better structural representation of the aircraft in study, but it can be considered the worst of the 3 Geometric Models developed. To better explain it, this model uses only Shell FE, even for representing components that clearly behave as a beam. Examples of these components are the booms, the spars and the vertical tail. This fact leads to a mandatory increase of the FE's thickness of these components, to compensate the bad capability of these elements to behave as a beam. This way, it is not possible to lower more the weight without compromising the constrains defined, specially δ_{tail}.

Finally, the Beam-Shell Geometric Model was developed in order to try to take advantage of both models advantages - it allows an accurate representation of the entire structure's geometry and it uses Beam FEs for the components that behave as beams and it uses Shell FEs for the components that behave as shells. Running the SIM on top of this Geometric Model produces a weight of $2190.46kg$, which falls in between the values obtained for the other two Geometric Models, as expected. Among the 3, this is definitely the model that should produce the more accurate results, due to the reasons defined.

However, even using the BSGM, the weight obtained is yet a bit higher than the goal weight of $1500kg$. This is due to the fact that, for simplicity, only 14 variables were considered for the definition of the Geometric Model, meaning that only 14 geometric parameters could be changed. By defining other variables, a lower weight could have been achieved. As an example, considering a higher wing skin thickness near the wing root and a thinner thickness near the tip, using a $t\_wingshell\_root$ and a $t\_wingshell\_tip$ variables, could lead to a decrease of the weight (i.e. tapering the skin thickness). Also, using the same approach on the booms could have also been possible. In short, the increase of the model complexity would benefit of an increase of the variables number, in order to obtain a reduced structural weight. However, this increase felt of the scope of the project, but it is definitely something that could be tested in future work.

One other parameter that is worth evaluating is the time per simulation of each Geometric Model, to understand the efficiency of each one. The results collected are presented in Table 14.

Table 14: Time spent per simulation.

Model	Static [s]	Mass [s]
Beam	16.21	6.61
Shell	14.59	6.42
Beam-Shell	33.62	12.76

The Beam and the Shell Geometric Models have quite low simulation times, either for the Static and Mass simulations. The higher values of the Static simulation are mostly due to the need for applying the aerodynamic forces on the wing and tail components, which is a process that really slows down the simulation.

The Beam-Shell Geometric Model has much higher values when compared with the other two. This is essentially due to the complexity of the model, which needs to couple 3 different types of FE (BEAM189, SHELL281 and MASS21) and has also a huge number of FEs: 32392 against 573 for the BGM and 3444 for the SGM. This adds an extra computational effort when defining and resolving the matrices that define the FEM problem, leading to an higher simulation time.

Regarding the SIM itself, it presents really good results. It was capable of reducing the initial weights of Beam, Shell and Beam-Shell Geometric Models in 76.46%, 48.12% and 61.40% indicating

that it is a reliable model. Also, the model can be applied to any type of Geometric Model and with any type of constrains, making it appealing for future studies.

In Table 15 the advantages and disadvantages of each Geometric Models developed are presented.

Table 15: Advantages and Disadvantages of each Geometric Model.

Modes	Advantages	Disadvantages
BGM	• Simple to develop • Computationally efficient • Less Variables • Allows a first simple and quick visualization of the forces acting on the structure	• Does not allow a correct representation of the Geometry, since some components can not be represented • Weight obtained is underestimated • Model might produce inaccurate results • Wrong usage of Beam FE in the ribs
SGM	• Simple to develop • Computationally efficient • Less Variables • It allows a better representation of the geometry	• Wrong usage of Shell FEs in several components, such as spars and booms • Weight obtained is clearly overestimated, due to the wrong usage of Shell FEs in all the components • Model might produce inaccurate results
BSGM	• Accurate representation of the Geometry and all the components • More accurate results • Correct usage of different FEs according to the type of component	• More complex model, leading to more variables • Higher time spent per simulation

5. Conclusion

The main objectives of this work were achieved, since three different Geometric Models were developed, using ANSYS APDL, each one of them with a different degree of complexity, that allow the study and analysis of the Flexcraft structure. These models can be used to determine the behavior of the structure, due to the effects of inertial and aerodynamic loading. They were also prepared for parametrization processes, since several geometric values are defined as variables and must be introduced beforehand.

Due to the above, a SIM was also developed, which can run on top of each Geometric Model. This is an algorithm that changes the input variables, according to the values defined in the start. A FEA is made for each different variation, being the needed results exported for analysis.

With this algorithm, is then possible to obtain an approximation of an optimized structure, that withstands the aerodynamic and inertial loads, without overcoming some geometric and structural constrains that are defined during the project phase and must be passed in the beginning of the SIM.

The SIM can be implemented in any other Geometric Model built using ANSYS APDL, as long as the Geometric Model is prepared for parametrizations. This fact shows the great versatility of this Parametric Model, which is one of its biggests assets, along with the ease of use.

References

[1] F. Afonso, H. Policarpo, F. Lau, and A. Suleman. Desenvolvimento - Projeto de VRP, FLEXCRAFT E.3.1. Report, Instituto Superior Técnico, Lisbon, Portugal, 2018.

[2] F. Afonso, J. Vale, F. Lau, and A. Suleman. Performance based multidisciplinary design optimization of morphing aircraft. *Aerospace Science and Tecnology*, 67:1–12, August 2017.

[3] ANSYS, Inc, Southpoite 275 Technology Drive Canonsburg, PA 15317. *Theory Reference for the Mechanical APDL and Mechanical Applications*, peter kohnke edition, April 2009. Release 12.0.

[4] K.-J. Bathe. *Finite Element Procedures*. K.J. Bathe, Watertown, MA, 2nd edition edition, 2016. ISBN 978-0-9790049-5-7.

[5] T. C. Corke. *Design of Aircraft*. Pearson Education, Upper Saddle River, N.J.: Prentice Hall, November 2002. ISBN 0-13-089234-3.

[6] J. J. M. da Silva. Design and optimization of a wing structure for a UAS Class I 145 kg. Master's thesis, Técnico Lisboa, July 2017.

[7] C. C. Ike. Timoshenko beam theory for the flexural analysis of moderately thick beams – variational formulation, and closed form solution. -*Italian Journal of Engineering Science*, 63(1):34–45, March 2019.

[8] A. Kale, E. Acart, R. T. Haftka, and W. J. Stroud, editors. *Why are Airplanes so Safe Structurally? Effect of Various Safety Measures on Structural Safety of Aircraft*. 45th AIAA/ASME/ASCE/AHS/ASC Structures, Structural Dynamics and Materials Conference, April 2004.

[9] J. Katz and A. Plotkin. *Low-Speed Aerodynamics*. Cambridge University Press, 2nd edition edition, 2001. ISBN 978-0-521-66219-2.

[10] J. G. Kaufman and E. L. Rooy. *Aluminum Alloy Castings: Properties, Processes, and Applications*. ASM International, December 2004.

[11] Y. Kaushik. A review on use of aluminium alloys in aircraft components. *Journal on Material Science*, 3(3):33–38, December 2015.

[12] G. Liu and S. Quek. *The Finite Element Method - A Practical Course*. Butterworth-Heinemann, 2nd edition, 2014. ISBN 978-0-08-098356-1.

[13] T. M. Salih. Nature of the materials for modern airplane parts. 12 2010.